Chem. Eng. Technol. **2009**, *32*, No. 9, 1403–1410

Petra M. Prechtl[1]
Lioubov Kiwi-Minsker[1]
Dmitri A. Bulushev[1]
Bryan K. Bromley[1]
Albert Renken[1]

[1] Ecole Polytechnique Fédérale de Lausanne, Lausanne, Switzerland.

Research Article

N_2O Decomposition over Fe-ZSM-5 Studied by Transient Techniques

Dedicated to Prof. Dr.-Ing. Gerhart Eigenberger on the occasion of his 70th birthday

N_2O decomposition to gaseous N_2 and O_2 catalyzed by a commercial Fe-ZSM-5 has been studied by different transient techniques: *(i)* via the transient response methods at ambient pressure, *(ii)* via the temporal analysis of products (TAP) reactor under vacuum, and *(iii)* by temperature-programmed desorption (TPD) under vacuum. The catalyst was activated in He at 1323 K. Two main steps can be distinguished within the transient period of N_2O decomposition under constant N_2O feed at 603 K: the first step consists of molecular N_2 formation and surface atomic oxygen $(O)_{Fe}$. It follows a period of stoichiometric N_2O decomposition to gaseous N_2 and O_2 with increasing conversion until steady state is reached. The observed rate increase is assigned to a slow accumulation on the surface of $NO_{x,ads}$ species formed from N_2O and participating as co-catalyst in the N_2O decomposition. The $NO_{x,ads}$ species accelerates the atomic oxygen recombination/desorption, which is the rate-determining step of N_2O decomposition. The formation and accumulation of $NO_{x,ads}$ species during N_2O interaction with the catalyst was confirmed by TAP studies. The amount of $NO_{x,ads}$ was found to depend on the number of N_2O pulses injected into the TAP reactor. In the presence of adsorbed NO_x on the catalyst surface ($NO_{x,ads}$) the desorption of dioxygen is facilitated. This results in a shift of the oxygen desorption temperature from 744 K to considerably lower temperatures of 580 K in TPD experiments. Pulses of gaseous NO had a similar effect leading to the formation $NO_{x,ads}$, thus facilitating the oxygen recombination/desorption.

Keywords: Fe-containing HZSM-5; N_2O decomposition; NO; Temperature-programmed desorption; Temporal analysis of products

Received: May 12, 2009; *revised:* June 11, 2009; *accepted:* June 17, 2009

DOI: 10.1002/ceat.200900248

1 Introduction

N_2O is an environmental pollutant since it is a greenhouse gas with a warming potential 310 times higher than that of CO_2, and its concentration in the atmosphere is still on the rise. ZSM-5 zeolites containing iron are known as promising catalysts in the nitrous oxide decomposition to gaseous N_2 and O_2 [1–8].

At 523 K only the formation of surface atomic oxygen $(O)_{Fe}$ on Fe-containing sites and gaseous N_2 from N_2O takes place. Molecular oxygen appears in the gas-phase only at higher temperatures indicating that the recombination/desorption of atomic oxygen from the catalyst surface is the rate-limiting step in N_2O decomposition [9–11]. The addition of gaseous NO enhances the activity of Fe-containing zeolites especially at low temperatures < 623 K [9, 11–15]. Slow NO formation from N_2O and accumulation on the catalyst surface is observed over Fe- and Cu-zeolites [16–20]. Nitro/nitrous [11, 14, 21] as well as nitrite/nitrate [22, 23] redox cycles are proposed for the active sites regeneration.

Perez-Ramirez et al. [11] studied the N_2O decomposition over homemade isomorphously substituted ex-framework Fe-ZSM-5 (~0.66 % Fe) with the Multi-Track, a temporal analysis of products (TAP)-like system. It was supposed that adsorbed NO may accommodate oxygen loaded from N_2O on an adjacent site, allowing the deposition of a second oxygen and helping the recombination of both. Adsorbed NO may even

---

Correspondence: Prof. Dr. Albert Renken (albert.renken@epfl.ch), EPFL-ISIC, Station 6, CH-1015 Lausanne, Switzerland.

facilitate the migration of atomic oxygen enhancing their recombination and desorption. They observed NO-induced NO_2 desorption while they did not report formation of $NO_{x,ads}$ species from N_2O in the absence of added gaseous NO.

The TAP multifunctional reactor [24] is a suitable technique to dose precisely reactants, to minimize homogeneous gas-phase reactions due to the Knudsen diffusion regime, and to dehydroxylate the catalyst under vacuum. Hydroxylation is well known to affect the ZSM-5 activity for N_2O decomposition [17, 25, 26] rendering more difficult mechanistic observations, which can be minimized in the TAP reactor under vacuum and at small amounts of reactants.

In this work, an increasing N_2O decomposition rate with time was observed by the transient response method at ambient pressure. Temperature-programmed desorption (TPD) and pulse response experiments were performed under vacuum in the TAP reactor with a conventional Fe-ZSM-5 to provide a more detailed understanding of the increasing catalyst activity and to gain supplementary mechanistic information on the N_2O decomposition.

2 Experimental

2.1 Catalyst

The Fe-ZSM-5 zeolite used in the present study was kindly provided by Zeochem AG (Uetikon, Switzerland). The powder with Si/Al = 25 was found to contain 5500 ppm of iron as an impurity. The high Fe content originates from the binder used for the formation of extrudates. The zeolite was calcined in a flow of He for 1 h at 1323 K for activation. The fraction of iron sites involved in the formation of surface oxygen $(O)_{Fe}$ from N_2O was measured via transient response methods during N_2O decomposition over the catalyst at 523 K. The concentration of active sites was in the range of $2.6–3.4 \cdot 10^{18}$ sites·g^{-1}. The main characteristics of the zeolite and the determination of active sites are described in detail by Yuranov et al. [27].

2.2 Transient Response and TPD Measurements

The catalytic activity was characterized by the transient response method carried out in a Micromeritics AutoChem 2910 analyzer provided with a ThermoStar 200 (Pfeiffer Vacuum) quadrupole mass spectrometer to analyze the composition of the gas phase ($p < 10^{-2}$ Pa). The following mass-to-charge ratios were monitored simultaneously by the mass spectrometer: 4 (He), 18 (H_2O), 28 (N_2, N_2O), 30 (NO, N_2O), 32 (O_2), 40 (Ar), 44 (N_2O), 46 (NO_2). It was calibrated using gaseous mixtures of known compositions.

0.40 g of Fe-ZSM-5 was placed in a quartz plug-flow reactor. Before the measurements, the catalyst was pretreated in He (50 mL·min^{-1}) at 1323 K for 1 h, then cooled to the studied temperature (603 K). Transient response experiments were performed by switching the He flow to a mixture of 2 vol.-% N_2O/2 vol.-% Ar/96 vol.-% He at 20 mL (STP)·min^{-1} flow rate. Ar served as an inert tracer.

After the N_2O interaction and cooling to 523 K in He (50 mL·min^{-1}) a TPD was performed in the range of 523 to 1323 K with a 30 K·min^{-1} ramp. All gases were provided by Carbagas (Lausanne, Switzerland) and their purities were higher than 99.998 %.

2.3 Temporal Analysis of Products

The interactions of N_2O and NO with Fe-containing ZSM-5 and the surface species were investigated by multipulse, pump-probe, and temperature-programmed desorption (TPD) in vacuum experiments using a TAP-2 setup [24]. It consists of four main parts: a gas mixing station, a microreactor with four high-speed pulse valves, a vacuum system, and a mass spectrometer.

The tubular microreactor is constructed of stainless steel with an inner diameter of 6.4 mm and 31.8 mm length. The entrance of this reactor seals via a small volume against the valve-manifold assembly through an O-ring. The reactor outlet is continuously evacuated by an oil diffusion pump that is pumped by a mechanical pump. The pulse valves allow a rapid injection of very small amounts of reactant into the microreactor using typical pulses with durations between 80 and 200 µs. The responses of reactant and products are recorded as function of time with the quadrupole mass spectrometer (ABB Extrel) located directly at the reactor exit, thus working at the same pressure as the microreactor. Two gas blending stations serve to prepare different gas mixtures and to determine the amount of reactants in the gas pulse by means of a pressure transducer.

A catalyst bed of 50 mg of Fe-ZSM-5 was placed between two beds of quartz particles (200-250 µm) and exposed to vacuum ($< 10^{-5}$ Pa). The temperature in the reactor was measured by a thermocouple positioned in the center of the catalyst bed. TAP experiments were carried out at 523 K, 593 K, and 661 K with mixtures of 80 vol.-% N_2O/20 vol.-% Ar and 10 vol.-% NO/90 vol.-% Ar which were introduced by pulses in the microreactor. Argon was used as an internal standard for calibration. The amount of the nitrous oxide blend in the inlet pulse was typically $5 \cdot 10^{14}$ molecules (pulse width 150 µs) and for the NO mixture $6.5 \cdot 10^{14}$ molecules allowing the transport in the reactor to occur by Knudsen diffusion. Prior to the measurements, the catalyst was kept under vacuum in the TAP reactor at 946 K for 30 min, and then cooled down to the studied temperature. This pretreatment will be referred to as “standard” in this paper. Experiments were carried out at 523 K, 593 K, and 661 K.

Three different transient methods were applied:

(i) The reactants were introduced by repetitive pulsing every 3 s with mixtures of N_2O/Ar and NO/Ar. N_2O and NO interactions with the catalyst were carried out in general with 600 pulses at 523 K and 593 K.

(ii) Pump-probe experiments were performed at 661 K by pulsing a mixture of N_2O/Ar at 0 s and NO/Ar after variable time delays from 1 to 9.5 s. Two valves were used to pulse the reactants consequently and the total cycle time was fixed to 10 s.

(iii) Complementary, TPD experiments were carried out to gain information about adsorbed surface species. Hence, after a defined sequence of pulses the catalyst temperature was increased linearly with a ramp of 45 $K\cdot min^{-1}$ from the studied temperature up to 916 K in vacuum.

Ar (99.998 %), NO (99.90 %), and N_2O (99.0 %) were used without further purification. Depending on the type of experiment the following mass-to-charge (*m/e*) ratios were registered: 28 (N_2, N_2O), 30 (NO, N_2O), 32 (O_2), 40 (Ar), 44 (N_2O), 46 (NO_2).

3 Results

3.1 Catalytic Decomposition of N_2O Studied by Transient Response

The interaction of N_2O with the Fe-ZSM-5 catalyst at 603 K and ambient pressure was studied by transient response and the results are presented in Fig. 1. Nitrogen and oxygen were the only products observed. Nitrogen passed initially through a sharp maximum and then increased slowly while oxygen increased continuously. Nitrogen appeared simultaneously with Ar and N_2O was observed with a certain delay due to decomposition and reversible adsorption on the catalyst surface [28]. The simplified dynamics of the N_2O decomposition can be explained by two reaction steps. Initially, N_2O decomposes forming surface atomic oxygen $(O)_{Fe}$ and gaseous N_2 as seen in Fig. 1 during the first 60 s. In a second step the formation of molecular oxygen is observed. The increasing concentrations of N_2 and O_2 with time seen in Fig. 1 indicate a transition period with increasing catalyst activity reaching steady state after 23 min of reaction with a final conversion of around 20 %. The concentration of active Fe-sites ($2.6–3.4 \cdot 10^{18}$ $sites\cdot g^{-1}$) [27] corresponds to about 5% of the total Fe concentration in the sample. A subsequent TPD experiment at ambient pressure in a flow of He (not shown) revealed besides oxygen the formation of $NO_{x,ads}$ species desorbed as NO at temperatures > 673 K. In order to understand the reasons for the activity increase, a TAP reactor study was performed with the same catalyst.

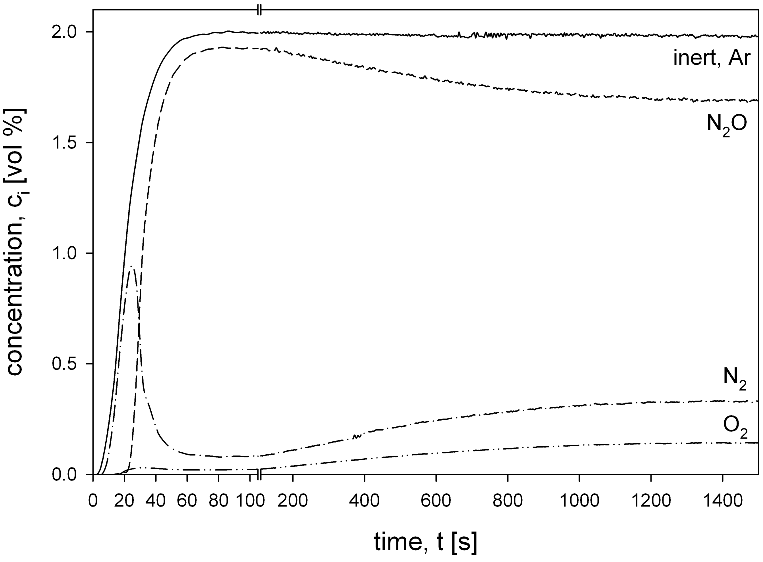

Figure 1. Transient response curves obtained during introduction of the 2 vol.-% N_2O, 2 vol.-% Ar mixture in He on the Fe-ZSM-5 catalyst at 603 K.

3.2 N_2O Interaction with Fe-ZSM-5 at Low Temperatures: TAP Coupled with TPD

Adsorbed surface species on the Fe-ZSM-5 catalyst were investigated by temperature-programmed desorption (TPD) experiments performed after different numbers of N_2O pulses at 523 K and 593 K in the TAP reactor. At these temperatures N_2O formed gaseous N_2 and atomic surface oxygen $(O)_{Fe}$ involving Fe-containing sites. The stoichiometric decomposition of N_2O to molecular oxygen and nitrogen in the TAP reactor was only observed at temperatures higher than 661 K. No gaseous NO/NO_2 was detected during pulsing N_2O in the range of 523 K to 946 K.

After N_2O pulsing over the zeolite at 593 K, only O_2 and NO were detected during the TPD runs. Nitrogen is very weakly adsorbed and desorbs immediately from the surface. Oxygen loaded during the N_2O interaction of 300, 600, and 1800 pulses was released within peaks at 713 K, 701 K, and 678 K, respectively (see Fig. 2a). The NO peaks observed during the TPD experiments are shown in Fig. 2b. Clearly seen is the increased amount of NO released from the surface with increasing number of performed N_2O pulses suggesting that NO was formed from N_2O. It is interesting to note that NO desorbed during the TPD experiments always at the very end of the oxygen desorption with the maxima at 707 – 757 K. The gaseous NO detected in the TPD runs are assigned to different surface NO_x species ($NO_{x,ads}$). They do not correspond to NO adsorbed originated from an impurity in the dosed N_2O blend since the accumulation of $NO_{x,ads}$ was not detected at pulse experiments performed at lower temperatures where adsorption phenomena should be strengthened. The results suggest the generation of $NO_{x,ads}$ species on the zeolite during N_2O decomposition. With increasing amount of accumulated $NO_{x,ads}$, the oxygen desorption temperature shifts to lower temperatures (~35 K) indicating easier recombination of atomic oxygen and desorption of O_2, as can be deduced from the theory of TPD processes [29].

At 523 K the loading of oxygen on iron sites from N_2O as well as the formation of $NO_{x,ads}$ were much slower. TPD runs after 600 N_2O pulses showed desorption of gaseous O_2, but no NO could be detected (see Fig. 3b, curve 1, Section 3.3). Nevertheless, the desorption maxima of oxygen decreased as well (744 K to 730 K) with increasing number of N_2O pulses (600 to 1200, not shown) indicating the existence of surface $NO_{x,ads}$ on the catalyst.

The formation of $NO_{x,ads}$ from N_2O is in line with transient response experiments at ambient pressure (Section 3.1) where $NO_{x,ads}$ species were created during N_2O interaction. The data lead to

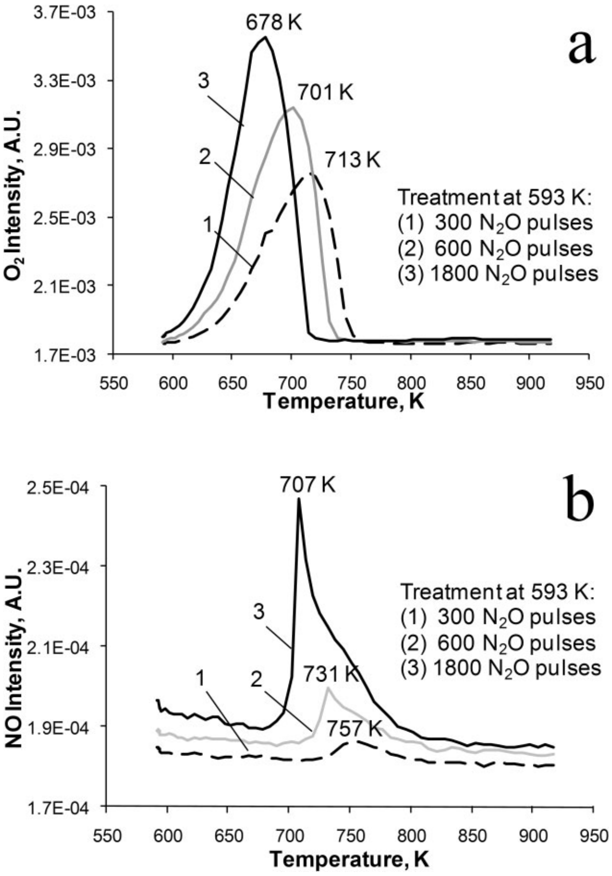

Figure 2. O_2 (a) and NO (b) TPD profiles after 300 (1), 600 (2), and 1800 (3) pulses of N_2O over the Fe-ZSM-5 catalyst at 593 K.

the assumption that the formed $NO_{x,ads}$ surface species enhance the desorption of $(O)_{Fe}$. To confirm this suggestion, experiments with preadsorption of gaseous NO were performed.

3.3 N_2O Interaction with Fe-ZSM-5 Containing Preadsorbed NO

The number of performed NO pulses was kept constant at 600 and the reaction temperature was set at 523 K in the following experiments. Under these conditions, the consecutive N_2O pulsing did not lead to the saturation of the catalyst with atomic oxygen. N_2O pulses over the catalyst with preadsorbed NO did not provoke the NO desorption while surface oxygen from N_2O was loaded. The TPD profiles were compared after three different catalyst treatments: *(i)* N_2O pulses; *(ii)* NO pulses → N_2O pulses, *(iii)* N_2O pulses → NO pulses → N_2O pulses. The number of pulses for each compound was 600. The consequent O_2 TPD profiles are presented in Fig. 3a. The maximum of the oxygen desorption shifted strongly to lower temperatures from 744 K (treatment 1) to 646 K and to 580 K (treatments 2 and 3). The amount of deposited $(O)_{Fe}$ doubled after the preadsorption of NO (see Fig. 3a, curve 2) and was six times bigger after $N_2O \rightarrow NO$ pretreatment (see Fig. 3a, curve 3) compared to the first experiment without preadsorption of NO (see Fig. 3a, curve 1).

Fig. 3b illustrates the corresponding TPD profiles for NO. No detectable NO was seen in TPD after N_2O pulsing (curve 1) in contrary to the pretreated catalyst with NO (curve 2) and $N_2O \rightarrow NO$ (curve 3). The $NO_{x,ads}$ species desorbed each time at the very end of the oxygen desorption as a sharp NO peak similar to those formed during the N_2O interaction with the catalyst at 593 K, as discussed in Section 3.1. Curves 3 and 4 of Fig. 3b show the responses for the mass-to-charge ratio (*m/e*) 30 (NO and NO_2) and *m/e* 46 (NO_2) during the TPD after the $N_2O \rightarrow NO \rightarrow N_2O$ multipulse sequences with their maxima at 611 K. Thus, it can be suggested that also NO_2 was desorbed from the catalyst in TPD runs.

The increased amount of $NO_{x,ads}$ species after different treatments as shown in Fig. 3b is in line with NO TPD results shown in Fig. 4. The amount of desorbed NO was very small after standard treatment and 600 NO pulses as seen in the NO-TPD profile (see Fig. 4, curve 1). In contrast, the sample with preloaded oxygen from N_2O desorbed NO in bigger amounts (see Fig. 4, curve 2) which was accompanied by desorption of NO_2 (see Fig. 4, curve 3).

The amount of loaded $(O)_{Fe}$ increased with increasing concentration of $NO_{x,ads}$ species on the catalyst (see Fig. 3), while NO_{ads} was not known to significantly enhance oxygen loading from N_2O when studied by the transient response method under normal pressure [21]. This observation can be explained by the transport of molecules into the micropores of the catalyst at low pressure [30–32]. Adsorption within the pores can only occur by diffusion of molecules adsorbed at the exterior surface of the zeolite particles. An accelerated surface diffusion of adsorbed oxygen will lead to a faster liberation of active sites on the outer surface, thus increasing the adsorption capacity of the zeolite.

An enhanced surface oxygen migration due to NO_{ads} was suggested in [11], which would in TAP experiments increase the amount of free active sites on the outer surface of the catalyst and explain the augmentation of $(O)_{Fe}$ formation through N_2O interaction with increasing NO_{ads}.

In summary, the effect of addition of gaseous NO to N_2O stream is the enhanced formation of $NO_{x,ads}$ species which decreased the oxygen desorption maximum in TPD runs. Isothermal studies were also performed to confirm the facilitated oxygen desorption by $NO_{x,ads}$ species. Due to the weak adsorption of N_2, the amount of adsorbed nitrogen is negligible.

3.4 NO Interaction with Fe-ZSM-5 Containing Preloaded Oxygen $(O)_{Fe}$

N_2O/NO pump-probe experiments were performed over the Fe-ZSM-5 catalyst at 661 K. N_2O pulses were repeated every 10 s. Besides N_2O alone, NO was injected after different time delays. After 10 to 20 cycles the response curves were identical as shown in Fig. 5. At the working temperature of 661 K oxygen desorbed slowly evolving as a very broad peak after each N_2O pulse (see Fig. 5, curve 1).

To study the effect of NO on the N_2O decomposition, pulses of N_2O and NO were consecutively fed to the reactor. A pulse

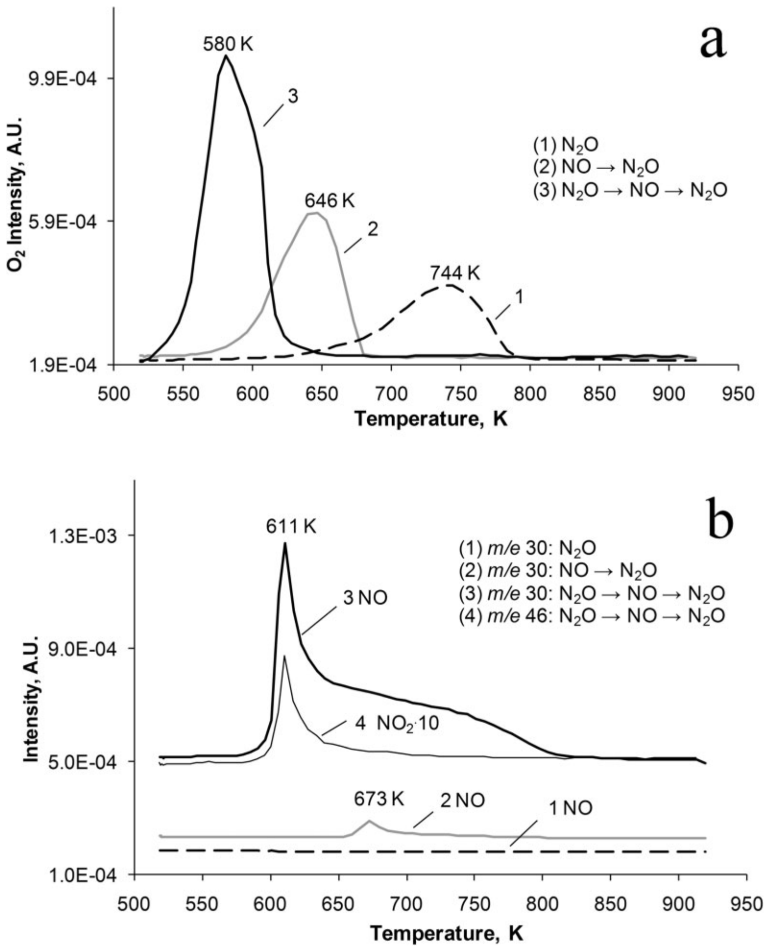

Figure 3. O_2 (a) and NO/NO_2 (b) TPD profiles after pulsing N_2O (1), NO → N_2O (2), N_2O → NO → N_2O (3), and NO_2 TPD profile after pulsing N_2O → NO → N_2O (b, 4) over the Fe-ZSM-5 catalyst at 523 K.

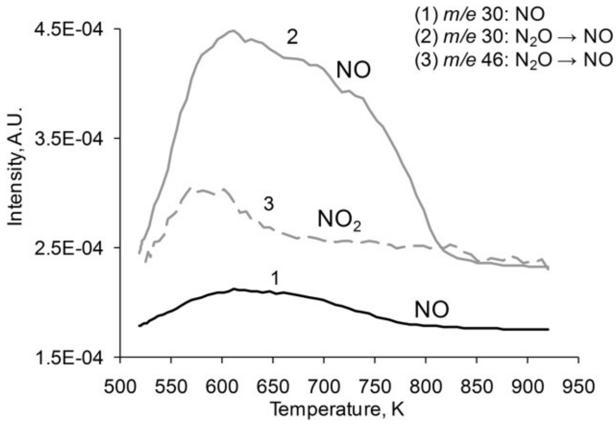

Figure 4. NO TPD profile after pulsing NO (1) and N_2O → NO (2), NO_2 TPD profiles after pulsing N_2O → NO (3) over the Fe-ZSM-5 catalyst at 523 K.

of N_2O was followed by a pulse of NO. The time interval between the two pulses was varied from 1 to 9.5 s and the alternate pulsing was repeated in cycles of 10 s. The oxygen responses are exemplified in Fig. 5 for a delay time of 1 s (curve 2), 4 s (curve 3), and 9.5 s (curve 4). The amount of evolved oxygen per cycle was independent of the time interval between the N_2O and the NO pulse. In the case of 1 s (curve 2) and 4 s (curve 3) delay time, NO was introduced when the oxygen from the previous N_2O pulse was still in the adsorbed state. This caused the appearance of an additional very sharp O_2 peak during the NO pulse. This peak was not observed when Ar was pulsed instead of NO. It was not accompanied by nitrogen or NO_2 evolution. No gaseous NO_2 was detected during the reaction under any reported conditions in contrary to the results of Pérez-Ramírez et al. [11]. Decomposition of NO to N_2 and O_2 was also never observed. The NO response over the $(O)_{Fe}$ free catalyst was very broad (not shown). Initial sharpening of the oxygen response was observed especially when the NO pulse was short-time before the N_2O pulse as in Fig. 5, curve 4 with 0.5 s between the NO and N_2O pulses (9.5 s between the N_2O and NO pulses). This suggests that the pulsed NO is in an adsorbed state as $NO_{x,ads}$ species before the N_2O pulse arrived. Switching off the NO pulsing resulted in NO desorption and transition of the catalyst behavior to the original one, with a very broad O_2 response like that shown in Fig. 5, curve 1.

It was shown earlier that the atomic oxygen from N_2O is loaded very quickly and there is no O_2 re-adsorption on the Fe-ZSM-5 catalyst [9, 11, 21]. Hence, the shape of the O_2 response is due to the O_2 desorption as the rate-determining step during the N_2O decomposition. Thus, the desorption of oxygen from the Fe-ZSM-5 is accelerated by pulses of NO. Molecular oxygen at 661 K desorbs very slowly without the assistance of NO, while at temperatures lower than 600 K the desorption of oxygen is negligible. Therefore, it is interesting to investigate the interaction of NO with the oxygen loaded from N_2O (600 pulses) at lower temperatures of 593 K. The coverage of the active iron sites with atomic oxygen was in all experiments low and far from saturation.

NO pulses over the $(O)_{Fe}$ preloaded catalyst at 593 K (600 pulses of N_2O) provoked the desorption of gaseous O_2, as illustrated in Fig. 6. After a first sharp oxygen peak, further oxygen desorption is observed over the whole cycle of 3 s. The desorption rate increases with increasing number of NO pulses and seems to reach a plateau after ca. 40 pulses. The desorption rate diminishes after ca. 70 pulses due to the exhaustion of adsorbed oxygen $(O)_{Fe}$. A strong irreversible adsorption of NO during the first pulses was also observed experimentally (not shown).

4 Discussion

Thermal pretreatment in vacuo or He as used in the present work creates extraframework Fe^{2+} sites [33–36], which are sup-

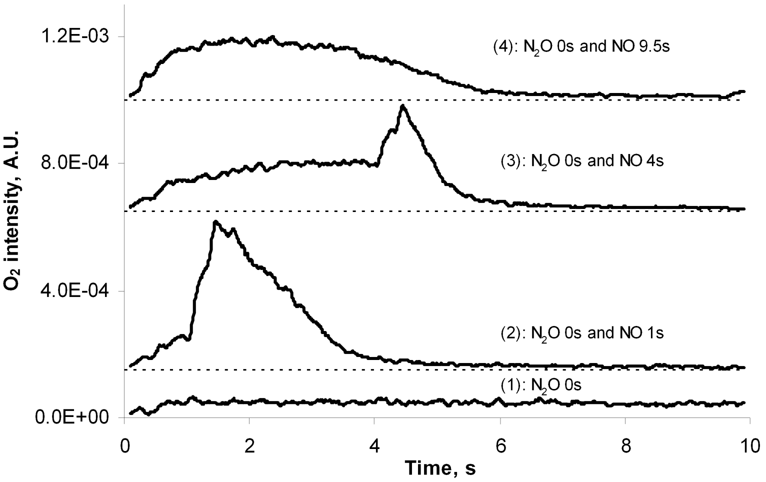

Figure 5. O_2 response from N_2O pulse at 0 s (1), N_2O pulse at 0 s and NO pulse at 1 s (2), N_2O pulse at 0 s and NO pulse at 4 s (3), and N_2O pulse at 0 s and NO pulse at 9.5 s (4) over Fe-ZSM-5 at 661 K.

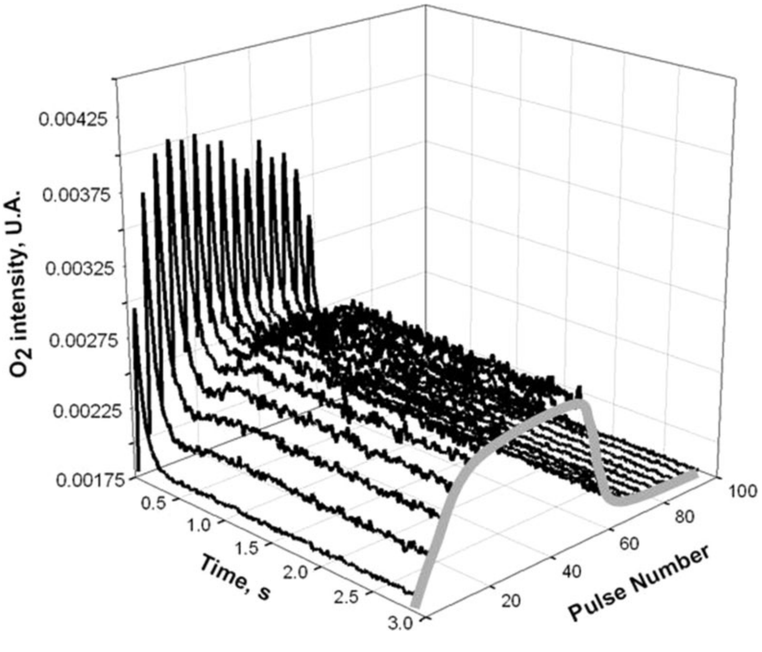

Figure 6. Oxygen desorption from the Fe-ZSM-5 provoked by NO pulses at 593 K after $(O)_{Fe}$ deposition from N_2O. Gray line: guide for eyes.

posed to be the active sites involved in the N_2O decomposition to gaseous N_2 and O_2 .

An increased activity of Fe-ZSM-5 in N_2O decomposition with time on stream at constant N_2O feed (2 vol.-%) was observed at ambient pressure (see Fig. 1). Surface $NO_{x,ads}$ species were found upon N_2O interaction with the catalyst. They play a key role in N_2O decomposition and were further studied in the TAP reactor in vacuum. At 593 K N_2O interacted with FeZSM-5 forming surface atomic oxygen $(O)_{Fe}$ and gaseous N_2 while molecular oxygen was not observed in TAP studies at temperatures lower than 660 K. The formation and accumulation of surface $NO_{x,ads}$ species was evidenced by TPD performed after the N_2O interaction with the catalyst (see Fig. 2 b).

Following the results of Bulushev et al. [16], a simplified scheme of the N_2O interaction with Fe-ZSM-5 at low temperatures can be suggested:

$$N_2O_{gas} \rightleftarrows N_2O_{ads}$$
(reversible adsorption, instantaneous) (1)

$$N_2O_{ads} + (\ )_{Fe} \longrightarrow N_2 + (O)_{Fe}$$
(deposition of atomic oxygen) (2)

$$2(O)_{Fe} \longrightarrow O_2$$
(recombination of oxygen, desorption; slow) (3)

$$N_2O + (O)_{Fe} \longrightarrow 2NO_{ads} + (\ )_{Fe}$$
(formation of surface NO) (4)

Due to the absence of inhibition of the N_2O decomposition by NO and the fact that NO appears as a result of the N_2O pulses in the TAP reactor, a competition of NO and loaded oxygen for the same sites can be excluded.

Pump-probe at 661 K as well as multipulse experiments at lower temperatures (523 and 593 K) showed that the desorption of molecular oxygen is facilitated by pulses of NO. TPD in vacuum and transient response experiments at ambient pressure also confirm that accumulated $NO_{x,ads}$ species promote the atomic oxygen recombination and O_2 desorption.

In addition, the O_2 desorption maximum was shifted in the TPD profile to lower temperature as the $NO_{x,ads}$ species amount on the catalyst increased. Thus, the rate-determining step, the recombination and desorption of surface atomic oxygen [9-11] is promoted by adsorbed $NO_{x,ads}$ species (Figs. 3a and b). Different but adjacent sites for NO adsorption and surface atomic oxygen formation from N_2O are proposed. Adsorbed NO may be further oxidized to NO_2 species acting as a co-catalyst in N_2O decomposition.

The catalytic action of NO can be explained by the reaction with surface oxygen as shown below:

$$NO_{ads} + (O)_{Fe} \longrightarrow NO_{2,ads} + (\ )_{Fe}$$
(formation of surface NO_2) (5)

$$NO_{2,ads} + (O)_{Fe} \longrightarrow NO_{ads} + (O_2)_{Fe}$$
(formation of surface di-oxygen) (6)

$$(O_2)_{Fe} \longrightarrow O_2 + (\ )_{Fe} \quad (7)$$

N_2O/NO pump-probe experiments showed also the promoting effect of NO on the oxygen recombination/desorption at 603 K. At this temperature oxygen desorption usually took place very slowly (see Fig. 5, curve 1). It is interesting to note that pulsing NO on a partly oxygen-loaded catalyst provokes a short oxygen pulse as seen in Fig. 5, curves 2 and 3. This phenomenon is even more pronounced after complete saturation of the surface with $(O)_{Fe}$ followed by NO pulses as shown in Fig. 6.

NO pulses provoked a very sharp oxygen peak at the moment of NO injection, followed by a constant O_2 release over the following part of the cycle of 3 s. An increasing number of pulses leads to the accumulation of adsorbed $NO_{x,ads}$ species, thus promoting O_2 recombination/desorption. After ca. 20 pulses the constant oxygen desorption was nearly doubled compared to the first cycle and stayed constant over the next ca. 40 cycles. The exhaustion of $(O)_{Fe}$ leads finally to the extinction of O_2 desorption (see Fig. 6).

As an attempt to explain these observations, we suggest a fast recombination of atomic oxygen in the neighborhood of the newly adsorbed NO. The constant rate following the first sharp O_2 peak may be explained by the enhanced mobility of surface oxygen via intermediate formation of $NO_{2,ads}$ species as suggested by Perez-Ramirez et al. [11]. The transfer of oxygen from one adsorbed $NO_{x,ads}$ species to another until an isolated $(O)_{Fe}$ is reached and reaction (6) occurs, liberating dioxygen in step (7).

5 Conclusions

At 523 K, N_2O interacts with Fe ZSM-5 forming surface atomic oxygen $(O)_{Fe}$ and gaseous N_2 while molecular oxygen is not observed. Higher temperatures (661 K) lead to the production of gaseous oxygen, O_2 from N_2O, and conversion increased with time on the stream of N_2O. This increase was explained by $NO_{x,ads}$ species formed from N_2O and accumulated on the surface. The $NO_{x,ads}$ species acts as co-catalyst facilitating the oxygen recombination/desorption, the rate-determining step during the N_2O decomposition. TAP results in vacuum were in line with the observations from the transient response at ambient pressure.

TAP studies evidenced the formation and accumulation of $NO_{x,ads}$ during N_2O interaction with Fe-ZSM-5 as well as its effect to facilitate the oxygen desorption. Oxygen recombination/desorption steps involved in the catalytic N_2O decomposition were accelerated as a result of NO pulses at 661 K. Even at temperatures as low as 523 K NO provoked loaded oxygen desorption whereas in the absence of NO it was not observed. Pulses of NO did not block the sites for atomic oxygen loading from N_2O, but led to the creation of $NO_{x,ads}$ species. Two mechanisms seem to be involved: a fast of atomic oxygen in the neighborhood of the newly adsorbed NO and enhanced mobility of surface oxygen via intermediate formation of $NO_{2,ads}$ species. Contrary to the catalyst without preloaded $(O)_{Fe}$ (pretreated in the standard way), NO adsorbed in much more amounts in the presence of $(O)_{Fe}$ on the catalyst, confirming formation of $NO_{x,ads}$ species.

Acknowledgement

The assistance of Dr. J. T. Gleaves and Dr. R. Fushimi with the TAP setup is highly appreciated. We thank the Swiss Science Foundation for financial support (grant no: 200020-109452).

References

[1] B. M. Abu-Zied, W. Schwieger, A. Unger, *Appl. Catal., B* **2008**, *84 (1–2)*, 277.
[2] B. Bromley, V. Hessel, A. Renken, L. Kiwi-Minsker, *Chem. Eng. Technol.* **2008**, *31 (8)*, 1162.
[3] H. Guesmi, D. Berthomieu, L. Kiwi-Minsker, *J. Phys. Chem. C* **2008**, *112 (51)*, 20319.
[4] M. A. G. Hevia, J. Pérez-Ramírez, *Appl. Catal., B* **2008**, *77 (3–4)*, 248.
[5] K. Jisa et al., *J. Catal.* **2009**, *262 (1)*, 27.
[6] E. V. Kondratenko, V. A. Kondratenko, M. Santiago, J. Pérez-Ramírez, *J. Catal.* **2008**, *256 (2)*, 248.
[7] E. V. Kondratenko, J. Pérez-Ramírez, *Catal. Today* **2007**, *121 (3–4)*, 197.
[8] M. Rivallan et al., *Appl. Catal., B* **2008**, *84 (1–2)*, 204.
[9] D. A. Bulushev, L. Kiwi-Minsker, A. Renken, *J. Catal.* **2004**, *222 (2)*, 389.
[10] L. Kiwi-Minsker, D. A. Bulushev, A. Renken, *Catal. Today* **2005**, *110 (3–4)*, 191.
[11] J. Pérez-Ramírez, F. Kapteijn, G. Mul, J. A. Moulijn, *J. Catal.* **2002**, *208 (1)*, 211.
[12] G. Mul, J. Pérez-Ramírez, F. Kapteijn, J. A. Moulijn, *Catal. Lett.* **2001**, *77 (1–3)*, 7.
[13] P. Prechtl, *Ph.D. Thesis,* Ecole polytechnique fédérale de Lausanne **2007**.
[14] C. M. Sang, B. H. Kim, C. R. F. Lund, *J. Phys. Chem. B* **2005**, *109 (6)*, 2295.
[15] F. Kapteijn et al., *Stud. Surf. Sci. Catal.* **1996**, *101*, 641.
[16] D. A. Bulushev, A. Renken, L. Kiwi-Minsker, *J. Phys. Chem. B* **2006**, *110 (1)*, 305.
[17] E. M. El-Malki, R. A. v. Santen, W. M. H. Sachtler, *J. Catal.* **2000**, *196 (2)*, 212.
[18] G. Grubert, M. J. Hudson, R. W. Joyner, M. Stockenhuber, *J. Catal.* **2000**, *196 (1)*, 126.
[19] M. Shimokawabe, K. Tadokoro, S. Sasaki, N. Takezawa, *Appl. Catal., A* **1998**, *166 (1)*, 215.
[20] T. Turek, *Appl. Catal., B* **1996**, *9 (1–4)*, 201.
[21] D. A. Bulushev, A. Renken, L. Kiwi-Minsker, *J. Phys. Chem. B* **2006**, *110 (22)*, 10691.
[22] C. M. Sang, C. R. F. Lund, *Catal. Lett.* **2001**, *73 (1)*, 73.
[23] M. Rivallan, G. Ricchiardi, S. Bordiga, A. Zecchina, *J. Catal.* **2009**, *264 (2)*, 104.
[24] J. T. Gleaves, G. S. Yablonskii, P. Phanawadee, Y. Schuurman, *Appl. Catal., A* **1997**, *160 (1)*, 55.
[25] P. K. Roy, G. D. Pirngruber, *J. Catal.* **2004**, *227 (1)*, 164.
[26] I. Yuranov, A. Renken, L. Kiwi-Minsker, *Appl. Catal., A* **2005**, *281 (1–2)*, 55.
[27] I. Yuranov, D. A. Bulushev, A. Renken, L. Kiwi-Minsker, *J. Catal.* **2004**, *227*, 138.

[28] L. Kiwi-Minsker, D. A. Bulushev, A. Renken, *J. Catal.* **2003**, *219 (2)*, 273.

[29] J. L. Falconer, J. A. Schwarz, *Catal. Rev. – Sci. Eng.* **1983**, *25 (2)*, 141.

[30] J. A. Delgado, T. A. Nijhuis, F. Kapteijn, J. A. Moulijn, *Chem. Eng. Sci.* **2004**, *59 (12)*.

[31] V. Fierroet al., *Chem. Eng. J.* **2002**, *90 (1–2)*.

[32] O. P. Keipert, M. Baerns, *Chem. Eng. Sci.* **1998**, *53 (20)*.

[33] K. A. Dubkov et al., *J. Catal.* **2002**, *207 (2)*, 341.

[34] R. Joyner, M. Stockenhuber, *J. Phys. Chem. B* **1999**, *103 (29)*, 5963.

[35] L. J. Lobree, I. C. Hwang, J. A. Reimer, A. T. Bell, *Catal. Lett.* **1999**, *63 (3–4)*, 233.

[36] G. D. Pirngruber, P. K. Roy, *Catal. Today* **2005**, *110 (3–4)*, 199.